

Case Report

Detection of Abdominal Lymph Node Metastasis from Pancreatic Neuroendocrine Tumor by Somatostatin Receptor Scintigraphy: Comparison with Somatostatin Receptor Type 2 Immunostaining

Kazuhiro Kitajima^a Hideyuki Shiomi^b Takako Kihara^c Seiko Hirono^d
Ryota Nakano^b Tomohiro Okamoto^d Chisako Yagi^e Hirotugu Eda^f
Kosuke Matsuda^a Michiko Hatano^a Makoto Yoshida^c Hiroshi Kono^c
Seiichi Hirota^c Tetsuya Minami^g Koichiro Yamakado^a

^aDepartment of Radiology, Hyogo Medical University, Nishinomiya, Japan; ^bDivision of Gastroenterology and Hepato-Biliary-Pancreatology, Department of Internal Medicine, Hyogo Medical University, Nishinomiya, Japan; ^cDepartment of Surgical Pathology, Hyogo Medical University, Nishinomiya, Japan; ^dDepartment of Hepato-Biliary-Pancreatic Surgery, Hyogo Medical University, Nishinomiya, Japan; ^eDepartment of Diabetes, Endocrinology and Clinical Immunology, Hyogo Medical University, Nishinomiya, Japan; ^fDivision of Gastroenterology and Hepatology, Department of Internal Medicine, Hyogo Medical University, Nishinomiya, Japan; ^gDepartment of Radiology, Kanazawa Medical University, Uchinada, Japan

Keywords

Neuroendocrine neoplasm · Lymph node metastasis · Somatostatin receptor scintigraphy · Fluorodeoxyglucose positron emission tomography

Abstract

We report a 58-year-old male with a histopathologically proven grade 2 (G2) pancreatic neuroendocrine neoplasm and multiple abdominal node metastases by use of a laparoscopic pancreatic body and tail resection procedure, plus abdominal lymph node dissection. A primary pancreatic tail neuroendocrine tumor sized 20 × 25 mm was detected by contrast-enhanced computed tomography, somatostatin receptor scintigraphy (SRS), and fluorodeoxyglucose positron emission tomography (FDG-PET) examinations and pathologically diagnosed as a pancreatic neuroendocrine tumor (PNET, G2) based on positive immunostaining for somatostatin receptor (SSTR) type 2. Of three metastatic histopathological lymph nodes, two measured

18 × 21 and 10 × 12 mm, respectively, with whole strong SSTR immunostaining showing moderate uptake in SRS findings, whereas the other node, sized 8 × 10 mm, had strong SSTR immunostaining only in a small 6 × 6-mm-sized portion and showed no uptake in SRS findings, likely because of the limited spatial resolution of scintigraphy. On the other hand, only the largest node (18 × 21 mm) was visualized by FDG-PET. SRS may be useful for metastatic lymph node diagnosis based on SSTR immunostaining, though a disadvantage is the spatial resolution limitation.

© 2023 The Author(s).
Published by S. Karger AG, Basel

Introduction

Isotope-imaging modalities have become increasingly utilized for management of neuroendocrine neoplasm (NEN) patients. Due to expression of multiple somatostatin receptors (SSTRs) in about 70% of NENs, functional imaging with a somatostatin analog is recommended as a standard procedure for staging of NEN patients, especially when targeting SSTRs with the highest affinity for subtype 2 [1, 2]. In this regard, somatostatin receptor scintigraphy (SRS) is used for evaluating SSTR expression in vitro, allowing for determination of NEN disease staging, including detection of the primary tumor, lymph node metastasis, and distant metastasis, as well as detection of disease recurrence, and finally for selecting candidate patients for peptide receptor radiometabolic treatment with yttrium-90 or lutetium-177, somatostatin analogs [3].

To the best of our knowledge, few reports regarding detection of lymph node metastasis associated with a pancreatic neuroendocrine tumor (PNET) by SRS have been presented. In the present study, findings obtained with contrast-enhanced computed tomography (CT), SRS with single photon emission computed tomography/computed tomography (SPECT/CT), and ¹⁸F-fluorodeoxyglucose positron emission tomography/computed tomography (FDG-PET/CT) of a PNET and lymph node metastasis, shown to be pathologically relevant by examination of a resected specimen, are presented.

Case Report

A 58-year-old male had a pancreas tail tumor incidentally discovered during a medical checkup and came to our hospital for a detailed examination and treatment. Diagnostic confirmation of PNET grade 2 (G2) was achieved based on endoscopic ultrasound-fine needle aspiration pathological findings. LDH, NSE, and ProGRP in laboratory results were within normal limits. Preoperative contrast-enhanced CT showed a persistently enhanced mass in the pancreas tail that measured 20 × 25 mm (Fig. 1a,b), significantly enlarged #11p (18 × 22 mm) (Fig. 1a) and #18 (10 × 12 mm) lymph nodes (Fig. 2a), and an equivocal #11d node (8 × 10 mm) (Fig. 1a). Whole-body SRS with SPECT/CT scanning demonstrated abnormal uptake in the primary tail tumor (Fig. 1c), as well as the #11p (Fig. 1c) and #18 (Fig. 2b) nodes, while the #11d node showed no uptake in SRS findings (Fig. 1c). Whole-body FDG-PET/CT scanning showed mild FDG uptake with a maximum standardized uptake value of 2.89 in the primary tail tumor (Fig. 1d) and mild FDG uptake with a maximum standardized uptake value of 3.42 in the #11p node (Fig. 1d), with the #11d (Fig. 1d) and #18 (Fig. 2c) nodes showing no FDG uptake. No distant metastatic lesion was indicated by SRS with SPECT/CT or FDG-PET/CT findings, and the clinical stage was determined to be T2N1M0.

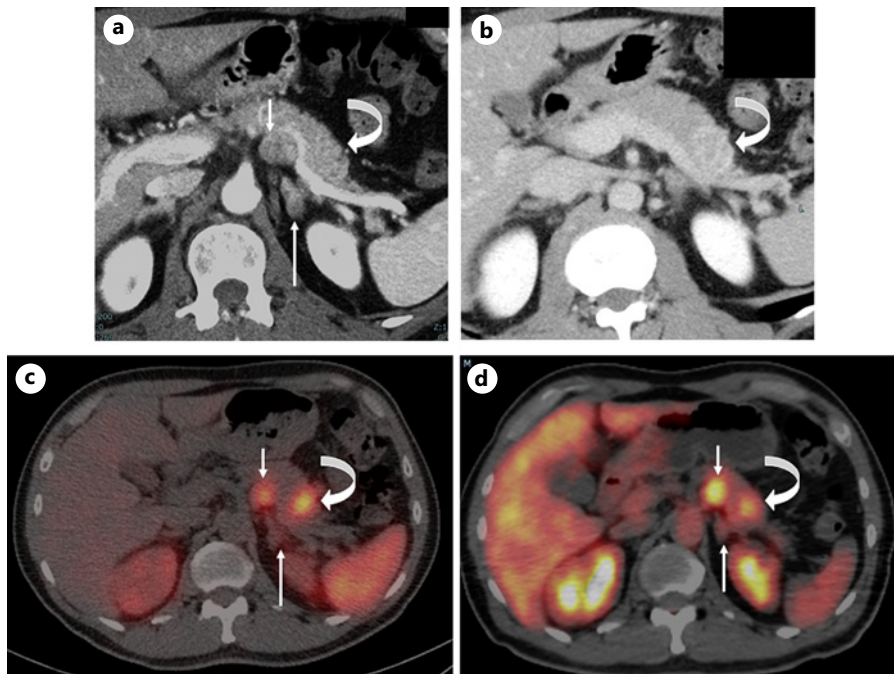


Fig. 1. CT, SRS with SPECT/CT, and FDG-PET/CT findings of NEN tumor metastasis in primary pancreatic tail and #11p and #11d lymph nodes. **a, b** Contrast-enhanced CT showed a persistently enhanced mass measuring 20 × 25 mm in the pancreas tail (curved arrow), a significantly enlarged #11p node measuring 18 × 22 mm (short arrow), and vague findings in the #11d node measuring 8 × 10 mm (long arrow). **c** SRS with SPECT/CT showed abnormal uptake in the primary tail tumor (curved arrow) and #11p node (short arrow), whereas there was no abnormal uptake in #11d node (long arrow). **d** FDG-PET/CT showed mild FDG uptake with a maximum standardized uptake value (SUVmax) of 2.89 in the primary tail tumor (curved arrow) and mild uptake with an SUVmax of 3.42 in the #11p node (short arrow), whereas no uptake was seen in the #11d node (long arrow).

Physicians at the Department of Hepato-Biliary-Pancreatic Surgery performed a laparoscopic resection of the pancreatic body and tail (Fig. 3a), plus dissection of abdominal lymph nodes, which included #8 (common hepatic artery nodes), #10 (splenic hilum nodes), #11 (splenic artery nodes), and #18 (inferior pancreatic nodes). A pathologic examination of the tail tumor, sized 20 × 23 mm, revealed a PNET with tumor cells small to intermediate in size, which had formed sheets and nests (G2) (Fig. 3b). Immunohistochemical findings with chromogranin A, synaptophysin, and somatostatin were positive, and the Ki-67 index was 5% (Fig. 3c–e). Pathological analyses of the lymph nodes showed that none of three in #8, none of four in #10, one (13 × 19 mm) of four in #11p, one (7 × 9 mm) of two in #11d, and one (8 × 12 mm) of three in #18 were metastatic. SSTR results of the primary tumor (Fig. 3f) showed positive staining, indicating three metastatic nodes: all of #11p, part (6 × 6 mm) of #11d, and all of #18 (Fig. 4a–c).

Discussion

A PNET is the second most common type of pancreatic tumor and represents a heterogeneous group of neoplasms with varying types of clinical expression and biological behavior, from indolent to aggressive. These tumors can be functioning or nonfunctioning in accordance with their ability to produce metabolically active hormones. PNET cases are

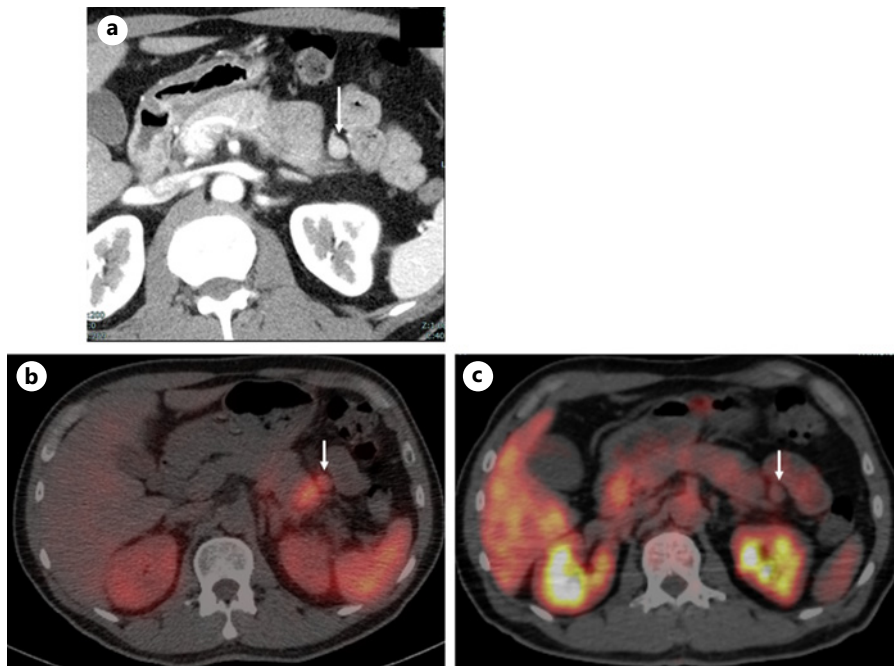


Fig. 2. FDG-PET/CT and SRS with SPECT/CT findings of #18 lymph node metastasis. **a** Contrast-enhanced CT showed a significantly enlarged #18 node measuring 10 × 12 mm (arrow), suggesting nodal metastasis. **b** SRS with SPECT/CT showed abnormal uptake in the #18 node (arrow), suggesting nodal metastasis. **c** FDG-PET/CT showed no FDG uptake in the #18 node (arrow).

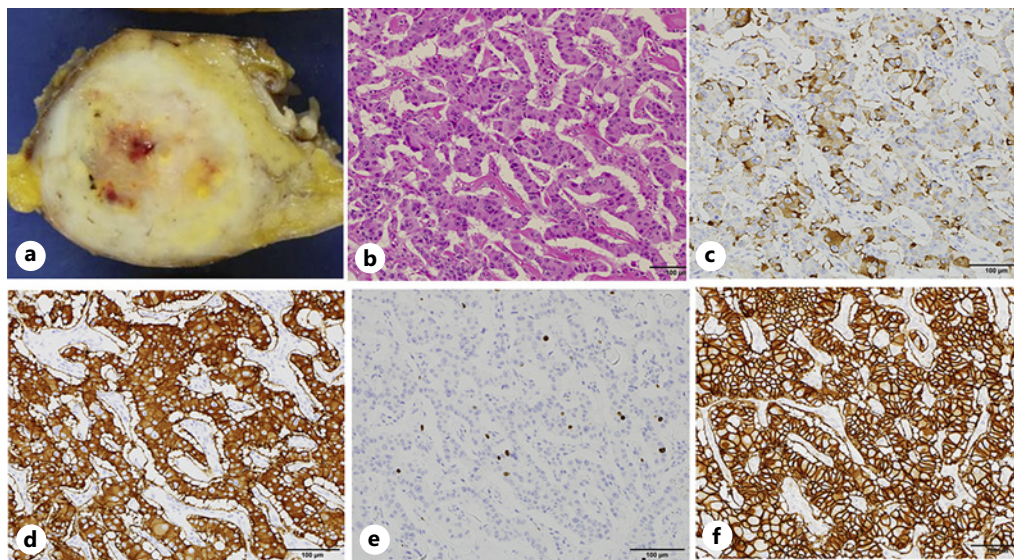


Fig. 3. Resected specimen and pathologic findings of primary tumor. **a** A tumor occupying nearly all of the pancreatic tail was revealed in the resected specimen. **b** Hematoxylin and eosin staining of a section of the specimen showed tumor cells small to intermediate in size, which had formed sheets and nests, and contained small round hyperchromatic nuclei with indistinct nucleoli and scanty cytoplasm. **c–e** Immunohistochemical findings with chromogranin A (**c**) and synaptophysin (**d**) were positive, while the Ki-67 index (**e**) was 5%. **f** Immunohistochemical findings with SSTR were positive.

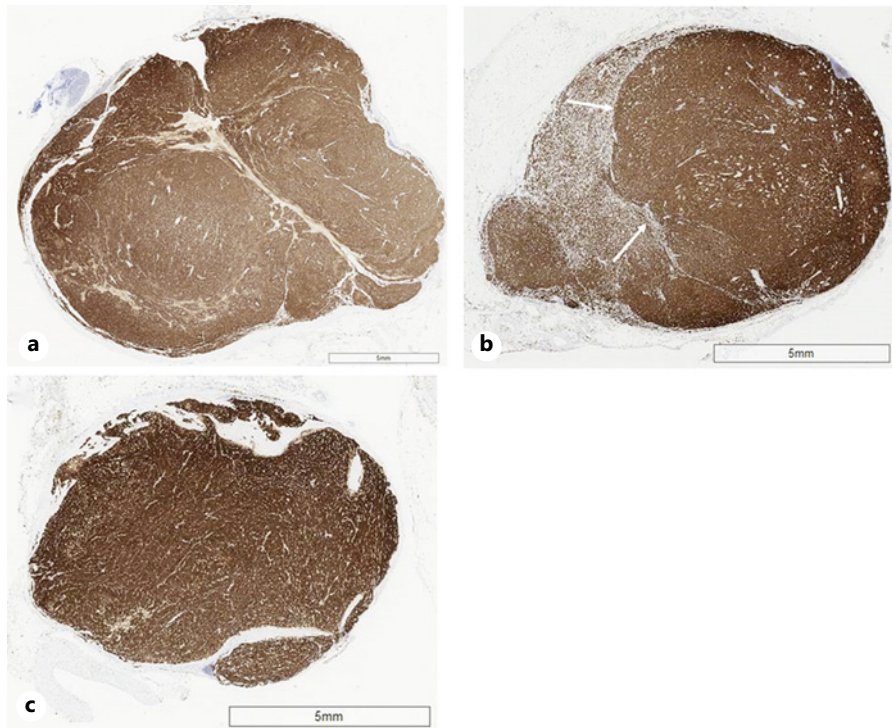


Fig. 4. Immunohistochemical findings with SSTR of three metastatic lymph nodes. The entire #11p node (13 × 19 mm) (a), part of the #11d node (6 × 6 mm) (b), and the entire #18 node (8 × 12 mm) (c) showed strong SSTR staining.

histopathologically classified according to the 2017 World Health Organization (WHO) classification system. Although the final diagnosis of neuroendocrine tumor relies on histologic results obtained in biopsy or surgical specimen examination results, both morphologic and functional imaging are crucial for patient care. Morphologic imaging with ultrasonography, CT, and magnetic resonance imaging, and functional imaging techniques with SRS and PET are useful for initial evaluations and disease staging, as well as surveillance and therapy monitoring.

SRS has been reported useful for detection, staging, and restaging of NEN cases, as well as therapy monitoring in light of SSTRs [4]. This functional technique is highly specific, with specificity found to range from 92% to 100% [5]. Other studies have shown sensitivity ranging between 40% and 70% [6], with better results for well-differentiated gastrinoma, glucagonoma, VIPoma, and nonfunctioning PNET as compared to poorly differentiated neuroendocrine carcinoma, insulinoma, or small-size NEN [4, 7].

By specifically targeting lesions with somatostatin receptors, SRS imaging might be helpful for identification of metastatic neuroendocrine tumor lesions, especially G1 and G2 types [8]. Kubota et al. [9] analyzed 15 patients with a total of 45 metastatic neuroendocrine tumor lesions and found an inverse correlation regarding the uptake of SRS and FDG tracers, as G1+2 lesions had a greater SRS uptake than G3 lesions, whereas the G1+2 lesions had a significantly lower FDG uptake as compared to G3 lesions. Those results were interesting, as a neuroendocrine carcinoma typically demonstrates a low level of SRS uptake.

Other metastatic sites for PNETs include the abdominal and mediastinal lymph nodes, peritoneum, and bone, more rarely the lungs, and even more rarely spleen, brain, thyroid, pituitary, breast, heart, meninges, and orbit tissues [3]. The frequency of metastatic site depends on the primary tumor, disease stage, and differentiation of the primary tumor. CT is

widely used as a first-line anatomical imaging method for initial tumor detection and staging, thanks to its availability, high spatial resolution, and rapid acquisition, while it is also more sensitive for detecting lung, liver, and peritoneal metastases, though SRS excels for exploring lymph nodes and bones [10, 11]. Magnetic resonance imaging is also useful to evaluate liver and bone metastases, as in addition to its high sensitivity, it is a non-radiant technique that can be repeated over time without risk of cumulative irradiation.

To the best of our knowledge, few reports have discussed detection of lymph node metastasis of PNET by SRS. Addeo et al. [12] compared contrast-enhanced CT with SRS for diagnostic accuracy of pathological lymph node metastasis from small bowel neuroendocrine tumors and found that the patient-based sensitivity of both was 46.7% (7 of 15). Furthermore, Binderup et al. [13] analyzed the diagnostic accuracy of SRS and FDG-PET in examinations of lymph node metastasis from several types of primary tumors and demonstrated that the sensitivity of SRS was better, though the difference was not significant ($p = 0.185$). Similar to those two studies, lesion-based sensitivity for pathological lymph node metastasis by CT and SRS was the same (2 of 3, 66.7%) in the present series and better than that of FDG-PET (1 of 3, 33.3%). SRS with moderate sensitivity of detecting metastatic lymph nodes is an important tool to decide surgical indication and decide a range of the lymph node dissection in NET patients in clinical situation. Unfortunately, SRS was not able to detect one small node with metastasis, as the area of strong SSTR immunostaining was only 6×6 mm, probably due to the limited spatial resolution of SPECT.

Conclusion

In the present PNET case, among three histopathological lymph nodes with metastasis shown positive by SSTRS (type 2) immunostaining, two nodes could be diagnosed using SRS findings, whereas one small metastatic node in which the area of strong SSTR immunostaining was only 6×6 mm could not be diagnosed, likely because of the limited spatial resolution of SPECT. SRS may be useful for determining metastatic lymph nodes in NEN cases based on SSTR, though a disadvantage is limited spatial resolution. It is important to be aware of both the advantages and disadvantages of SRS for imaging examinations of NEN patients. The CARE Checklist has been completed by the authors for this case report, attached as online supplementary material (for all online suppl. material, see <https://doi.org/10.1159/000531572>).

Statement of Ethics

This report complies with the guidelines for human studies and includes evidence that the research was conducted ethically in accordance with the World Medical Association Declaration of Helsinki. The authors have no ethical conflicts to disclose. Written informed consent was obtained from the patient for publication of this case report and any accompanying images. The paper is exempt from Ethical Committee approval because the Institutional Review Board of Hyogo Medical College of Medicine admits case reports without Ethical Committee approval.

Conflict of Interest Statement

The authors have no conflicts of interest to declare.

Funding Sources

No specific funding was received from any bodies in the public, commercial, or not-for-profit sectors to carry out the work described in this article.

Author Contributions

Concept, design, and drafting of the manuscript: K.K.; acquisition of data: H.S., T.K., S.H. (Seiko Hirono), R.N., T.O., C.Y., H.E., K.M., M.H., M.Y., H.K., S.H. (Seiichi Hirota), and T.M.; and critical revision of the manuscript for important intellectual content: K.Y. All authors approved the final version of the manuscript.

Data Availability Statement

All data generated or analyzed during this study are included in this article and its online supplementary material. Further inquiries can be directed to the corresponding author.

References

- 1 Papotti M, Bongiovanni M, Volante M, Allia E, Landolfi S, Helboe L, et al. Expression of somatostatin receptor types 1-5 in 81 cases of gastrointestinal and pancreatic endocrine tumors. A correlative immunohistochemical and reverse-transcriptase polymerase chain reaction analysis. *Virchows Arch*. 2002;440(5):461–75.
- 2 Koopmans KP, Neels ON, Kema IP, Elsinga PH, Links TP, de Vries EG, et al. Molecular imaging in neuroendocrine tumors: molecular uptake mechanisms and clinical results. *Crit Rev Oncol Hematol*. 2009;71(3):199–213.
- 3 Dromain C, Déandréis D, Scoazec JY, Goere D, Ducreux M, Baudin E, et al. Imaging of neuroendocrine tumors of the pancreas. *Diagn Interv Imaging*. 2016;97(12):1241–57.
- 4 Chiti G, Grazzini G, Cozzi D, Danti G, Matteuzzi B, Granata V, et al. Imaging of pancreatic neuroendocrine neoplasms. *Int J Environ Res Public Health*. 2021;18(17):8895.
- 5 Sundin A, Arnold R, Baudin E, Cwikla JB, Eriksson B, Fanti S, et al. ENETS consensus guidelines for the standards of care in neuroendocrine tumors: radiological, nuclear medicine & hybrid imaging. *Neuroendocrinology*. 2017;105(3):212–44.
- 6 Chougnat CN, Leboulleux S, Caramella C, Lumbroso J, Borget I, Déandréis D, et al. Frequency and characterization of gastro-entero-pancreatic neuroendocrine tumor patients with high-grade of uptake at somatostatin receptor scintigraphy. *Endocr Relat Cancer*. 2013;20(2):229–39.
- 7 Squires MH 3rd, Volkan Adsay N, Schuster DM, Russell MC, Cardona K, Delman KA, et al. Octreoscan versus FDG-PET for neuroendocrine tumor staging: a biological approach. *Ann Surg Oncol*. 2015;22(7):2295–301.
- 8 Kolasínska-Ćwikła AD, Konsek SJ, Buscombe JR, Maciejkiewicz K, Cichocki A, Roszkowska-Purska K, et al. The value of somatostatin receptor scintigraphy (SRS) in patients with NETG1/G2 pancreatic neuroendocrine neoplasms (p-NENs). *Nucl Med Rev Cent East Eur*. 2019;22:1–7.
- 9 Kubota K, Okasaki M, Minamimoto R, Miyata Y, Morooka M, Nakajima K, et al. Lesion-based analysis of (18)F-FDG uptake and (111)In-Pentetreotide uptake by neuroendocrine tumors. *Ann Nucl Med*. 2014;28(10):1004–10.
- 10 Dromain C, de Baere T, Lumbroso J, Caillet H, Laplanche A, Boige V, et al. Detection of liver metastases from endocrine tumors: a prospective comparison of somatostatin receptor scintigraphy, computed tomography, and magnetic resonance imaging. *J Clin Oncol*. 2005;23(1):70–8.
- 11 Leboulleux S, Dromain C, Vataire AL, Malka D, Aupérin A, Lumbroso J, et al. Prediction and diagnosis of bone metastases in well-differentiated gastro-entero-pancreatic endocrine cancer: a prospective comparison of whole body magnetic resonance imaging and somatostatin receptor scintigraphy. *J Clin Endocrinol Metab*. 2008;93(8):3021–8.
- 12 Addeo P, Poncet G, Goichot B, Leclerc L, Brigand C, Mutter D, et al. The added diagnostic value of ¹⁸F-fluorodihydroxyphenylalanine PET/CT in the preoperative work-up of small bowel neuroendocrine tumors. *J Gastrointest Surg*. 2018;22(4):722–30.
- 13 Binderup T, Knigge U, Loft A, Mortensen J, Pfeifer A, Federspiel B, et al. Functional imaging of neuroendocrine tumors: a head-to-head comparison of somatostatin receptor scintigraphy, 123I-MIBG scintigraphy, and 18F-FDG PET. *J Nucl Med*. 2010;51(5):704–12.